IOP Conf. Series: Journal of Physics: Conf. Series **1291** (2019) 012033 doi:10.1088/1742-6596/1291/1/012033

Effects of dissipative hydrodynamics on elliptic flow and HBT interferometry in central collisions at RHIC

D S Lemos[1] and O Socolowski Jr[2]

[1]Instituto de Física Teórica, Universidade Estadual Paulista, Brazil
[2]Instituto de Matemática, Estatística e Física, Universidade Federal do Rio Grande, Brazil

E-mail: dener.lemos@sprace.org.br

Abstract. In this work, we study relativistic heavy ion collisions by using a hydrodynamic model for both ideal and viscous cases to investigate the influence of dissipative effects on the elliptic flow and HBT interferometry. We conclude that the bulk viscosity has small influence in hydrodynamic calculations. However, our results show that the shear effects are important for describing the experimental data in central collisions.

1. Introduction

Relativistic heavy ion collisions allow the study of the behavior of matter under extreme pressure and temperature conditions. Under these conditions it is possible to observe a transition from ordinary matter to a quark-gluon plasma (QGP) [1]. One possible tool for studying the system formed in these collisions is the hydrodynamic model [2, 3]. The application of this model is based on the assumption that the system reaches a state of local thermodynamic equilibrium and in the fact that the matter formed in these collisions shows a collective behavior.

Our aim in this work is to investigate the influence of shear and bulk viscosities on elliptic flow and HBT radii by using a hydrodynamic model with smooth initial conditions and an equation of state based on lattice QCD with a crossover transition between the QGP and the hadron gas. The calculations were performed for central Au+Au collisions (0-5%) with $\sqrt{s_{\rm NN}} = 200$ GeV in 2+1 dimensions (boost invariance).

2. Hydrodynamic Model

In the hydrodynamic model each fluid element can be characterized by its energy-momentum tensor and other conserved numbers (baryonic number, strangeness, etc.). In this work, we assumed that all conserved numbers are zero, so the hydrodynamic equations can be written as

$$\partial_{;\mu} T^{\mu\nu} = \partial_\mu T^{\mu\nu} + \Gamma^\mu_{\sigma\mu} T^{\sigma\nu} + \Gamma^\nu_{\sigma\mu} T^{\mu\sigma} = 0, \tag{1}$$

where $\Gamma^\mu_{\sigma\mu}$ are the Christoffel symbols and $T^{\mu\nu}$ the energy-momentum tensor given by [4, 5]

$$T^{\mu\nu} = \epsilon u^\mu u^\nu - (P + \Pi)\Delta^{\mu\nu} + \pi^{\mu\nu}. \tag{2}$$

Here ϵ, u^μ, P, Π, $\pi^{\mu\nu}$ and $\Delta^{\mu\nu}$ are, respectively, the energy density, the fluid four-velocity, the pressure, the bulk viscosity, the shear viscosity tensor and the ortogonal projector to u^μ. We solved Eq. (1) in Milne coordinates [4].

The second order viscous hydrodynamic equations are calculated for both shear and bulk viscosities, using the Israel-Stewart framework [6]

$$\Delta^{\mu\alpha}\Delta^{\nu\beta}u^{\gamma}\partial_{;\gamma}\pi_{\alpha\beta} = -\frac{1}{\tau_{\pi}}\left[\pi^{\mu\nu}-\eta\sigma^{\mu\nu}\right]-\frac{4}{3}\pi^{\mu\nu}\partial_{;\gamma}u^{\gamma}, \quad (3)$$

$$u^{\gamma}\partial_{;\gamma}\Pi = -\frac{1}{\tau_{\Pi}}\left[\Pi-\zeta\partial_{;\gamma}u^{\gamma}\right]-\frac{4}{3}\Pi\partial_{;\gamma}u^{\gamma}, \quad (4)$$

where $\sigma^{\mu\nu}=\Delta^{\mu\lambda}\partial_{;\lambda}u^{\nu}+\Delta^{\nu\lambda}\partial_{;\lambda}u^{\mu}-\frac{2}{3}\Delta^{\mu\nu}\partial_{;\lambda}u^{\lambda}$ and η, ζ, τ_{π}, τ_{Π} are, respectively, the shear coeficient, the bulk coeficient, the shear relaxion time, the bulk relaxion time. The relaxion times depend on the viscous coeficiets as $\tau_{\pi}=\frac{3}{T}\frac{\eta}{s}$ and $\tau_{\Pi}=\frac{6}{T}\frac{\zeta}{s}$ [3], where T is the temperature and s the entropy density. The η/s and ζ/s are parameters in our model. To perform the hydrodynamic evolution, we also have to provide the initial conditions (IC) and the equation of state (EoS).

When the mean free path becomes of the order of the system size, the hydrodynamic model is no longer valid and the particles decouple by traveling in straight line to the detector. Here, we employ the freeze-out framework [7] to calculate the decoupling by using the Cooper-Frye formula [8]

$$\frac{1}{2\pi}\frac{dN}{p_{\mathrm{T}}dp_{\mathrm{T}}dyd\phi} = \int_{\Sigma}d\Sigma_{\mu}p^{\mu}f(p_{\mu}u^{\mu}), \quad (5)$$

where N is the number of particles, p_{T} the transverse momentum, y the rapidity, ϕ the azimuthal angle, p^{μ} the four-momenta and $d\Sigma_{\mu}$ is the normal vector to the freeze-out surface. The distribution function is given by $f=f_0+\delta f_{\pi}+\delta f_{\Pi}$, where f_0 is equilibrium distribution function [7]; δf_{π} and δf_{Π} are the corrections for shear and bulk viscosities, respectively [3].

3. Numerical Results

We used IC generated by T_RENTo [9]. The hydrodynamic equations were solved by using vHLLE [4] with the s95p EoS [10], and the decoupling calculated by using THERMINATOR2 [7]. We perform simulations for ideal fluids and different scenarios of viscous fluids. In viscous simulations we consider η/s constant in all the hydrodynamical evolution and ζ/s constant in the hadron gas phase and zero in the QGP phase [3].

3.1. Elliptic Flow

The collective behavior of the system formed in heavy ion collisions is described by the anisotropic flow [11], where the initial spacial anisotropy is reflected in the final state of particles. In order to calculate the anisotropic flow, we rewrite the azimuthal part in equation (5) using a Fourier tranform as

$$\frac{dN}{d\phi} = 1+2\sum_{n=0}^{\infty}v_n\cos\left(\phi-\psi_{\mathrm{R}}\right), \quad (6)$$

where v_n are the Fourier components and ψ_{R} is the reaction plane angle. Here, we calculated the second Fourier component (v_2), called elliptic flow, using the event plane method [12]. Figure 1 shows the p_{T} dependence of v_2 compared with data. The result for ideal hydrodynamics is shown in red line, the blue line is for viscous hydrodynamics with $\eta/s=0.08$ and $\zeta/s=0.04$, magenta line is for $\eta/s=\zeta/s=0.08$, green line is for $\eta/s=0.16$ and $\zeta/s=0.04$, and black squares are experimental data. We see that the ideal hydrodynamics can describe the data for $p_T<1$ GeV. However, for describing the data for higher values of p_T one has to include shear effects. Also, we can see that the bulk viscosity has no significant effects on v_2.

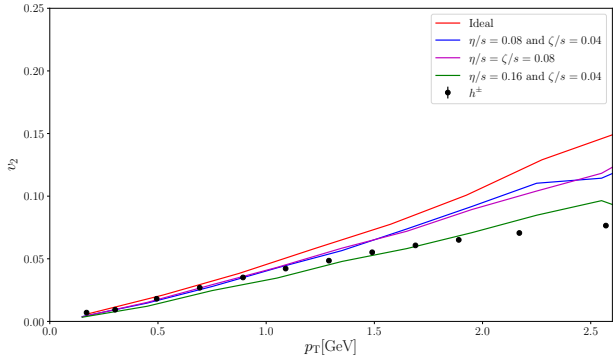

Figure 1. p_{T} dependence of v_2 for charged hadrons in central Au+Au collisions at 200 GeV. Comparison of ideal hydrodynamics and different viscous scenarios. Data from STAR collaboration [13]
.

3.2. HBT Interferometry

The HBT effect [15] allows measuring the space-time dimensions of the interacting region, at freeze-out, in a high energy collision. To calculate the so-called HBT radii, we used the correlation function defined, for a pair of pions with momentum p_1 and p_2, as

$$\mathcal{C}(p_1, p_2) = \frac{\mathcal{P}_2(p_1, p_2)}{\mathcal{P}_1(p_1)\mathcal{P}_1(p_2)}, \tag{7}$$

where $\mathcal{P}_2$ is the probability of detection of both particles simultaneously and $\mathcal{P}_1$ is the probability of detection of each particle individualy. We calculated the equation (7) using the Monte Carlo approach implemented in THERMINATOR2 by using the Berstch-Pratt coordinates [14]. The *long* coordinate is defined along the beam direction; the *out* coordinate is parallel to the average transverse momentum of the pair ($\vec{K}_{\mathrm{T}} = (\vec{p}_1 + \vec{p}_2)/2$) and the *side* coordinate is orthogonal to both *long* and *out*. We fitted the correlation function using a Gaussian function

$$\mathcal{C} = 1 + \lambda \exp\left\{-R^2_{out}q^2_{out} - R^2_{side}q^2_{side} - R^2_{long}q^2_{long}\right\}, \tag{8}$$

where $q = p_1 - p_2$ is the relative four-momentum of the pair in *out*, *side* and *long* directions and λ is the chaoticity parameter. Figure 2 shows K_{T} dependence of R_{out}, R_{side}, R_{long} and R_{out}/R_{side} for hydrodynamic simulations compared with data. The red-dashed line is the result for ideal hydrodynamics; the blue-dashed line is for viscous hydrodynamics with $\eta/s = 0.08$ and $\zeta/s = 0.04$; the magenta-dashed line is for $\eta/s = \zeta/s = 0.08$; the green-dashed line from $\eta/s = 0.16$ and $\zeta/s = 0.04$; black squares are experimental data. Although our results fail to reproduce the experimental data for R_{out}, R_{side}, and R_{long}, we can see no influence of bulk viscosity in HBT radii, analogously to v_2 results. We also have a better agreement with data for R_{out}/R_{side} when we increase the shear coeficient η/s.

4. Conclusions and Perspectives

In summary, we have used the hydrodynamic model in 2+1 dimensions for both ideal and viscous cases to calculate v_2 and HBT radii. We have shown that the effect of bulk viscosity is to small for both observables in central collisions. However, the inclusion of shear viscosity brings a better agreement with data for v_2 in higher p_{T} and for the ratio R_{out}/R_{side}. A more detailed study about the influence of dissipative effects can be found in [17]. Some improvements to this work can be made in the future: it includes hydrodynamic simulations in 3+1 dimensions, event-by-event initial conditions, viscous dependence on temperature.

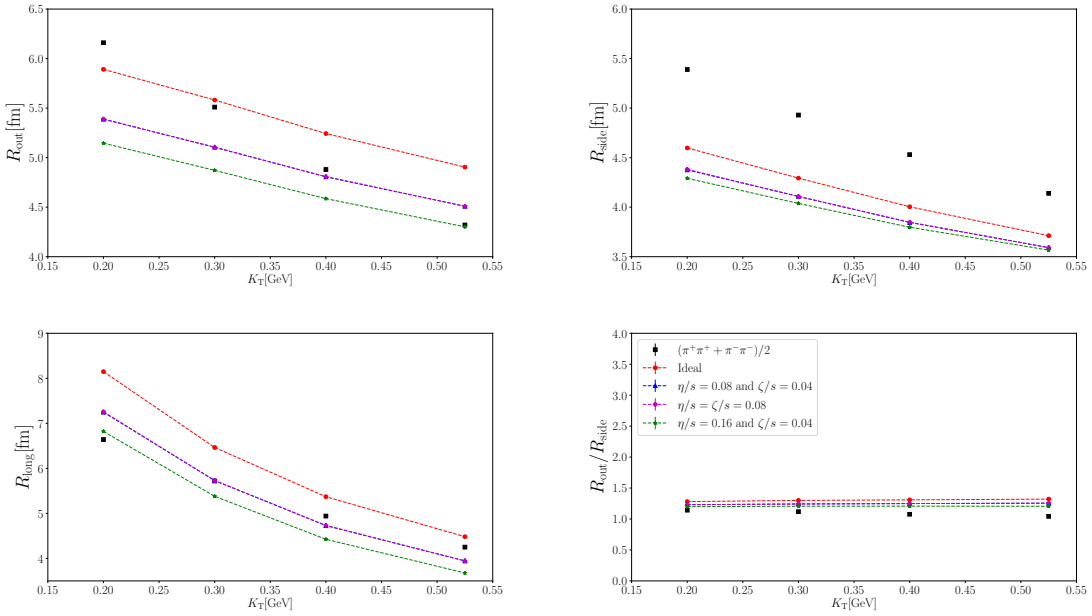

Figure 2. K_{T} dependence of HBT radii for charged pions in the Bertsch-Pratt system R_{out} (top left), R_{side} (top right), R_{long} (bottow left) and the ratio R_{out}/R_{side} (bottow right) for central Au+Au collisions at 200 GeV. Data from STAR collaboration [16].

5. Acknowledgments

This material is based upon work supported by the São Paulo Research Foundation (FAPESP) under Grant No. 2017/02675-6. This work was partially supported by CAPES (Brazilian research funding agency). This research was supported by computional resources supplied by the Center for Scientific Computing (NCC/GridUNESP) of the São Paulo State University (UNESP). DSL acknowledges the financial support by IFT/UNESP for participating in the XLI Brazilian Meeting on Nuclear Physics.

References

[1] Ludlam T and Aronson S 2005 Hunting the quark gluon plasma *BNL-73847-2005*.
[2] Hama Y, Kodama T and Socolowski Jr O 2005 *Braz. J. Phys.* **35** 24; Andrade R P G, Grassi F, Hama Y and Qian W L 2011 *Nucl. Phys.* A **854** 81; Noronha-Hostler J, Denicol G S, Noronha J, Andrade R P G and Grassi F 2013 *Phys. Rev.* C **88** 044916.
[3] Bozek P 2012 *Phys. Rev.* C **85** 034901.
[4] Karpenko Iu, Huovinen P and Bleicher M 2014 *Comp. Phys. Commun.* **185** 3016.
[5] Landau L D and Lifshitz E M 1987 Fluid Mechanics *Butterworth-Heinemann Ltd.*
[6] Israel W 1976 *Annals Phys.* **100** 310; Israel W and Stewart J M 1979 *Annals Phys.* **118** 341.
[7] Chojnacki M, Kisiel A, Florkowski W and Broniowski W 2012 *Comput. Phys. Commun.* **183** 746.
[8] Cooper F and Frye G 1974 *Phys. Rev.* D **10** 186;
[9] Moreland J S, Bernhard J E and Bass S A 2015 *Phys. Rev.* C **92** 011901.
[10] Huovinen P and Petreczky P 2010 *Nucl. Phys.* A **837** 26.
[11] Ollitrault J Y 1992 *Phys. Rev.* D **46** 229.
[12] Poskanzer A M and Voloshin S A 1998 *Phys. Rev.* C **58** 1671.
[13] STAR Collaboration 2005 *Phys. Rev.* C **72** 014904.
[14] Bertsch G F 1989 *Nucl. Phys.* A **498** 173C.
[15] Hanbury Brown R and Twiss R Q 1958 *Nature* **178** 4541; Padula Sandra S 2005 *Braz. J. Phys.* **35** 25;
[16] STAR Collaboration 2005 *Phys. Rev.* C **71** 044906.
[17] Lemos D S 2017 Efeitos da Hidrodinâmica Dissipativa e da Equação de Estado sobre o Fluxo Elíptico e a Interferometria HBT *Masters dissertation* FURG.